




## Warmer Antarctic summers in recent decades linked to earlier stratospheric final warming occurrences

Hyesun Choi <sup>1</sup>, Hataek Kwon<sup>2</sup>, Seong-Joong Kim <sup>1</sup>✉ & Baek-Min Kim <sup>3</sup>✉

Since the 2000s, the pause of the strong Antarctic cooling and later stratospheric final warming onset trends has been identified. Here we employ composite and congruence analysis using reanalysis and in-situ data to propose a linkage between pivotal changes in the surface temperature trends and the timing of stratospheric final warming events. In early stratospheric final warming events, the positive polar cap height anomaly developed in the stratosphere in early October, descending to the troposphere and surface in late spring and summer, resulting in high-pressure anomalies, which led to warmer surfaces in most of Antarctica. In late stratospheric final warming occurrences, opposing or weaker behaviors were observed. The trend toward earlier stratospheric final warming appears to play a considerable role in warmer summers over parts of interior Antarctica through the strengthening of the anti-cyclonic surface pressure anomaly. This could influence the regional sea-ice modulation over the Southern Ocean.

<sup>1</sup>Division of Polar Climate Sciences, Korea Polar Research Institute, Incheon, Republic of Korea. <sup>2</sup>School of Earth and Environmental Sciences, Seoul National University, Seoul, Republic of Korea. <sup>3</sup>Department of Environmental Atmospheric Science, Pukyong National University, Busan, Republic of Korea.  
✉email: [seongjkim@kopri.re.kr](mailto:seongjkim@kopri.re.kr); [baekmin@pknu.ac.kr](mailto:baekmin@pknu.ac.kr)

Observational evidence of the increasing loss of ice shelves in West Antarctica and sea ice in the Amundsen-Bellinghousen Sea over the 21st century has been reported<sup>1–5</sup>. As Antarctic ice mass loss is connected to the marine ecosystem and associated with the acceleration of global mean sea level rise<sup>3</sup>, polar region glacial changes are a regional and global-scale issue. The warming over western Antarctica has coincided with a decrease in Antarctic glaciers<sup>5</sup>.

Rapid reduction in Antarctic sea ice has drawn attention in recent years<sup>6–9</sup>. Antarctic sea ice loss can result in local impacts, such as Antarctic ice shelf disintegration and surface albedo changes<sup>6,7</sup>, as well as remote impacts, such as tropical warming and Arctic sea ice loss<sup>8,9</sup>. England et al. (2020b) showed that combined Arctic and Antarctic sea ice losses amplified global warming signals compared to the effects of only Arctic sea ice loss<sup>9</sup>.

Sea ice distribution and surface weather can be influenced by the direction and strength of atmospheric circulation and consequent anomalous cold and warm air advection<sup>1,10,11</sup>. Atmospheric circulation in the southern high latitudes can be modulated by various factors such as stratospheric ozone, stratospheric polar vortex strength, and internal variability of the climate system<sup>1,12–16</sup>. Tropical forcings such as El Niño–Southern Oscillation, Interdecadal Pacific Oscillation, and Pacific Decadal Oscillation also play an important role in the Antarctic surface temperature modulation<sup>2,17,18</sup>.

A stratospheric final warming (SFW) event is characterized by a final breakdown of the stratospheric polar vortex that occurs every spring<sup>19</sup>. The interannual variation in SFW occurrence timing largely modulates the year-to-year tropospheric variability of the Southern Annular Mode (SAM) and the seasonal evolution of eddy-driven jets during the austral summer<sup>20–23</sup>. The decadal variability of SFW occurrence timing is also an interesting issue. Rao and Garfinkel (2021) confirmed that future trends of SFW onset date (SFWOD) do not considerably differ from the present using model output<sup>24</sup>.

Previous studies<sup>19,22,25</sup> based on recent observational data, however, have reported that since the 2000s, the strong delay trend in SFWOD has been weakened and reversed to an advanced trend in the Southern Hemisphere (SH).

We noted a trend change in near-surface temperature during the austral summer over Antarctica in recent decades, as well as a change in the timing of SH SFW. This study examined the influence of a trend toward earlier SFW occurrences since the 2000s, on long-term variability in surface circulation, surface temperature, and sea ice in the SH, using both reanalysis and in situ observations. We propose that understanding the behavior of the SFW onset date can be a key factor in improving the forecasting skill of decadal and interannual variability of summertime surface weather over Antarctica. Results Section shows the composite behaviors in surface circulation and downward couplings according to SFW occurrence timing and differences in circulation trends related to the long-term variability of SFW occurrence timing. A summary and discussion are provided in Discussion Section. The data and methods employed in this study are described in Methods Section.

## Results

**Warmer Antarctic summers and earlier onset of stratospheric final warming.** Figure 1a shows the time series of December–January (DJ) mean surface air temperature (SAT) anomalies and SFWOD. The SAT anomalies were averaged over 10°W–270°E (90°W) and 70°S–90°S for the reanalysis data and calculated from 10 stations located in the 10°W–270°E (90°W) region for the observations. The selected areas for the average

SAT were Antarctica, excluding the Antarctic Peninsula (AP). The SAT anomalies based on reanalysis data (solid black line) and station observations (dashed-dotted black line) displayed a similar evolution, with a correlation coefficient of 0.86. On an interannual time scale, the two SAT anomalies from the reanalysis and observed data were related to SFWOD, with correlation coefficients of  $-0.34$  and  $-0.53$ , respectively, which are significant at a 95% confidence level using two-tailed Student's *t*-test. Thus, an earlier SFWOD is associated with warmer Antarctic surface temperatures during the austral summer season, and vice versa. Near-surface temperature anomalies and the SFWOD also exhibited long-term variability. The SAT anomaly based on reanalysis (station data) in Fig. 1a shows that the significant cooling trend with  $-0.43$  °C decade<sup>-1</sup> ( $-0.53$  °C decade<sup>-1</sup>) during the pre-1999 period reversed into an insignificant warming (cooling) trend with  $0.29$  °C decade<sup>-1</sup> ( $-0.004$  °C decade<sup>-1</sup>) during the post-1999 period at a 90% confidence level. The pre-1999 period and post-1999 periods were defined as 1979–1999 and 1999–2022, respectively. Note that the pause in the Antarctic cooling trend did not occur in austral winter (Supplementary Fig. 1 and Supplementary Note 1). The spatial patterns in the trend of SH SAT anomalies for the two eras showed approximately opposing behaviors (Fig. 1b, c). For the reanalysis data, the West and East Antarctic cooling trends and the AP warming trends during the pre-1999 period (Fig. 1b) were paused or slightly reversed during the post-1999 period (Fig. 1c). Owing to the contrasting trends in SAT anomalies between the AP and other Antarctic regions, the long-term variability in SAT anomalies over the entire Antarctic continent could be weakened through offsetting each other and veiling the SAT anomalies trend change in west and east Antarctica (Supplementary Fig. 2 and Supplementary Note 2). The results from the station observations (circles in Fig. 1b, c) were generally consistent with those from the reanalysis data.

The near-surface temperature anomaly trend change around 2000 coincided with the pause or slightly reversed trends of other SH near-surface circulation metrics, such as the mid-latitude jet position, SAM index, and Hadley cell edge<sup>13,14</sup>. A trend pause between the two periods was also observed in the SFWOD. At a 95% confidence level, a significant delay trend with  $+10.65$  d decade<sup>-1</sup> exhibited for the pre-1999 period paused into an insignificant delay trend with  $+0.53$  d decade<sup>-1</sup> for the post-1999 period. It is notable that excluding the last 3 years, during 1999–2019, a significant advance trend of  $-8.84$  d decade<sup>-1</sup> was observed with the 90% confidence level. A trend change in SFWOD before and after 21st century (or decadal variability in SFWOD) was also identified in another study<sup>22</sup>. In this study, we chose 1999 as the turnaround year. While the later occurrence of SFWOD for three consecutive years since 2020 weakened the advance trend, the periods before and after 1999 were considered as the SFWOD-delay and advance periods, respectively. We examined trends and differences between the pre- and post-intervention periods. The trend differences in SAT anomalies and SFWOD were insensitive to the turnaround year (Supplementary Table 1 and Supplementary Note 3).

**Antarctic climate features according to SFW timing.** Figure 2 shows the composite mean horizontal distributions of mean sea level pressure (MSLP) and SAT anomalies averaged over the austral summer (DJ) for early and late SFW events. A high-pressure anomaly developed during the early SFW events (Fig. 2a). In contrast, a low-pressure anomaly was prominent for late SFW events (Fig. 2b) over Antarctica, especially in the Antarctic Peninsula and the Amundsen and Ross Seas. The high-pressure anomaly over Antarctica, surrounded by the low-

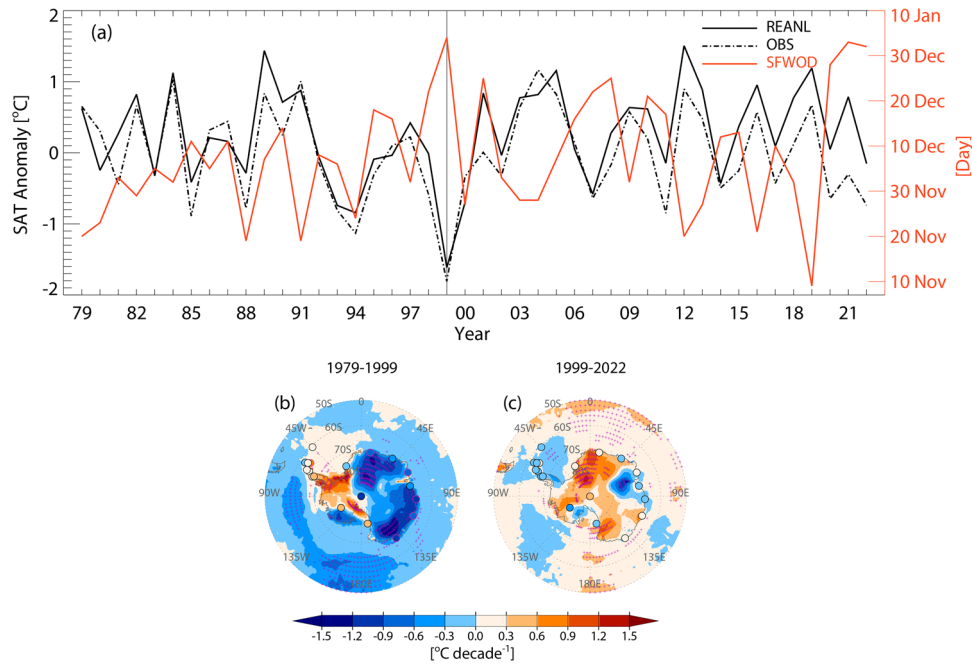


**Fig. 1 Time series of SAT anomalies and SFWOD, as well as spatial distributions of trends in SAT anomalies.** **a** Time series of DJ-mean SAT anomaly averaged over Antarctica excluding the AP region (black) and SFWOD (orange). The black solid and dashed-dotted lines correspond to the results from the reanalysis data and station observations, respectively. The vertical gray line represents the year 1999. Refer to the left axis for the DJ-mean SAT anomaly and the right axis for SFWOD. Spatial distribution of the DJ-mean SAT anomaly trends during **(b)** the pre-1999 (1979–1999) and **(c)** post-1999 (1999–2022) periods. The circles in **(b)** and **(c)** indicate the DJ-mean SAT anomalies for 20 Antarctic stations. Pink crosses and circles in Fig. 1b, c indicate significance at the 95% confidence level, respectively.

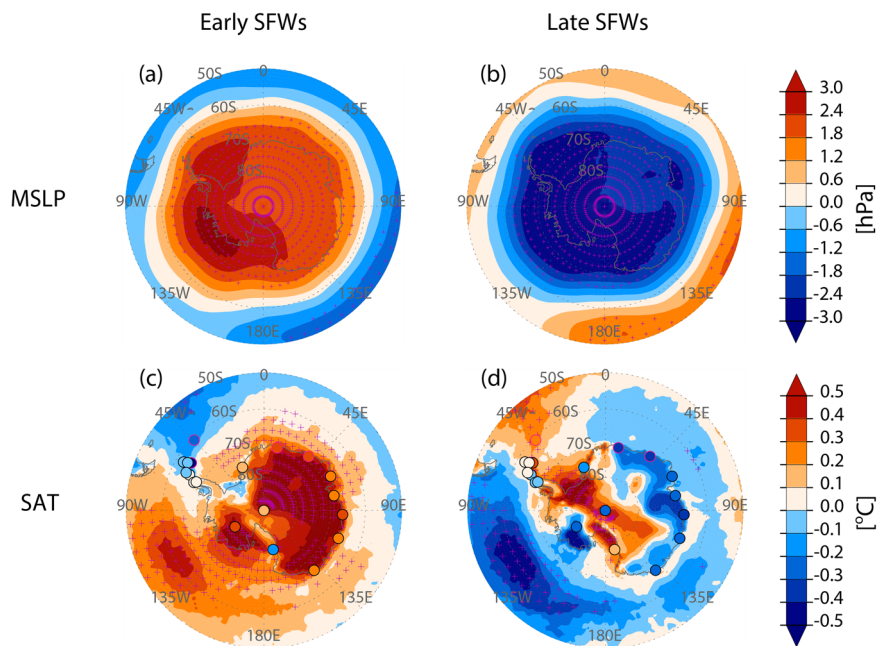


**Fig. 2 Spatial distributions of MSLP and SAT anomalies according to SFWOD.** DJ-mean MSLP anomalies for **(a)** the early-SFW and **(b)** late-SFW events. **c, d** are equivalent to **(a, b)** for DJ-mean SAT anomalies. The circles in **(c)** and **(d)** are the SAT anomalies for 20 Antarctic stations. Pink crosses and circles indicate significance at the 95% confidence level.

pressure anomaly over the Southern Ocean for early SFW events, resembles the negative phase of the SAM and vice versa<sup>22</sup>. This was confirmed by the significant positive correlation between SFWOD and the SAM index (Supplementary Fig. 3). The anti-cyclonic circulation anomaly over west Antarctica for early SFW events provided favorable conditions for cold air mass advection

to the AP region from the Antarctic continental interior, inducing a negative SAT. In contrast, the northerly circulation anomaly from the eastern Weddell Sea and Amundsen Sea was associated with a positive SAT anomaly over the rest of Antarctica (Fig. 2c). Cyclonic circulation anomalies for late SFW events drove almost opposing SAT responses over Antarctica, although they were less

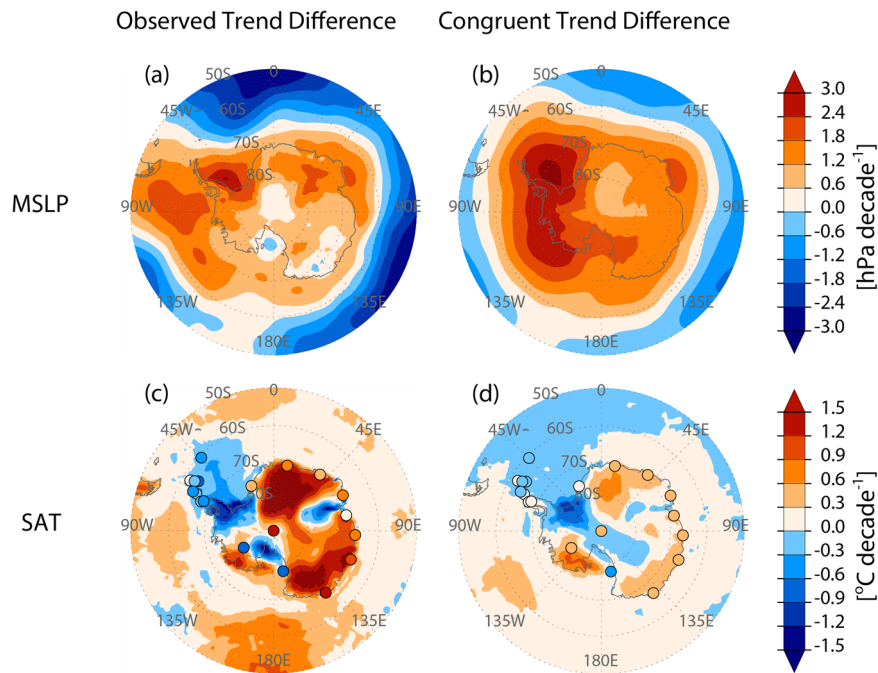


**Fig. 3 Spatial distributions of observed and congruent trend differences in MSLP and SAT anomalies.** **a** Trend differences between SFWOD-delay and advance period in DJ-mean MSLP anomaly (post-1999 period minus pre-1999 period). **b** is equivalent to **(a)** for trends linearly congruent with SFWOD. **c, d** are equivalent to **(a)** and **(b)**, respectively, for SAT anomalies. The circles in **(c)** and **(d)** are the DJ-mean SAT anomalies for 20 Antarctic stations.

robust in the Antarctic continental interior (Fig. 2d). The SAT anomaly composite results from the reanalysis data (shading in Fig. 2c, d) mostly agreed with the station observations (circles in Fig. 2c, d).

**Trend differences related to the SFWOD variability.** Figure 3a, c shows the spatial patterns of the differences in MSLP and SAT trends between the delayed and advanced periods in SFWOD. The positive trend difference in the MSLP anomaly over the Amundsen Sea and Antarctic continent (Fig. 3a) and the positive trend difference in the SAT anomaly over West and East Antarctica (Fig. 3c) strongly resemble those of early SFW events (Fig. 2a, c). This resemblance implicitly reflects the strengthening of prominent surface circulation and near-surface temperature patterns during the austral summer for the early SFW events, during the advanced period in SFWOD. We further examined the trend differences in the MSLP and SAT anomalies related to the long-term SFWOD variability. Figure 3b, d shows the changes in the surface circulation and temperature trends congruent with the SFWOD between the two eras. The similarity between the observed (Fig. 3a, c) and congruent trend differences (Fig. 3b, d) in terms of spatial patterns and amplitudes suggests that the signature of SFWOD substantially explains the observed trend differences in the MSLP and SAT anomalies over the SH high-latitude regions during the summer season. The results from the station observations (circles in Fig. 3c, d) are consistent with those from the reanalysis data. It is notable that the composite anomaly and the trend differences congruent with the SFWOD were insensitive to the removal of trends prior to the calculations (Supplementary Figs. 4–7). The fractions of trend differences related to the SFWOD in SAT anomalies in both the reanalysis and station observations were particularly pronounced in interior Antarctica compared to that in the AP, indicating regional differences in the signature of the SFWOD (Supplementary Fig. 8).

Given that the SFWOD is closely linked to large-scale circulation, such as the DJ-mean SAM phase (Supplementary Fig. 3), there may be a reasonable expectation that the short- and

long-term variability in Antarctic sea-ice concentration (SIC) can be attributed to surface wind and surface temperature driven by the SFWOD-related SAM. We explored the trend differences in the observed SIC and SIC anomalies linearly congruent with the SFWOD over Antarctica during the austral summer (Fig. 4). The regression coefficient between the DJ-mean SIC anomaly and SFWOD was calculated with the trend included, using the same method as in Fig. 3. The anti-cyclonic surface circulation over Antarctica, indicating a negative SAM phase, tended to strengthen during advanced periods in the SFWOD (Fig. 3a), inducing warm air mass advection to the Ross Sea and cold air mass advection to the Weddell Sea (Fig. 3c). Consequently, circulation anomalies can lead to a decrease in SIC over the northern Ross Sea and an increase in SIC over the AP region, as shown in Fig. 4a. The congruent trend differences in SIC (Fig. 4b) show strength and signs comparable to that of the actual trend differences in SIC over those regions, notably in the northern Ross Sea.

#### Differences in stratosphere-troposphere downward coupling.

To identify the relationship between surface temperature and stratospheric circulation according to the SFWOD, time-altitude cross-sections of the polar cap-height (PCH) anomaly were examined (Fig. 5). During the early SFW events (Fig. 5a), a positive PCH anomaly developed in the upper stratosphere in early October and began to propagate downward to the troposphere and surface in late spring and summer. Significant positive PCH anomalies continued intermittently at the surface from November to January. In contrast, during the late SFW events (Fig. 5b), the negative PCH anomaly propagated from the stratosphere to the surface. The significant signals in the troposphere and surface were more prominent before, rather than after, the mean onset of late SFW events. For late SFW events, prominent surface responses before the onset were also reported in a previous study. Byrne et al. (2017) confirmed that the high-latitude positive anomaly in the SH tropospheric zonal mean zonal wind showed a larger magnitude before, rather than after, the onset

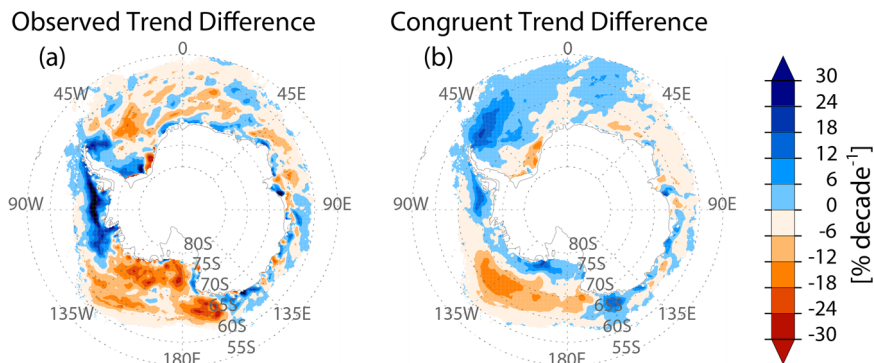


**Fig. 4** Spatial distributions of observed and congruent trend differences in SIC anomaly. **a** Trend differences between SFWOD-delay and advance period in DJ-mean SIC anomalies (SFWOD-advance era minus SFWOD-delay era). **b** is equivalent to **(a)** for trends linearly congruent with SFWOD.

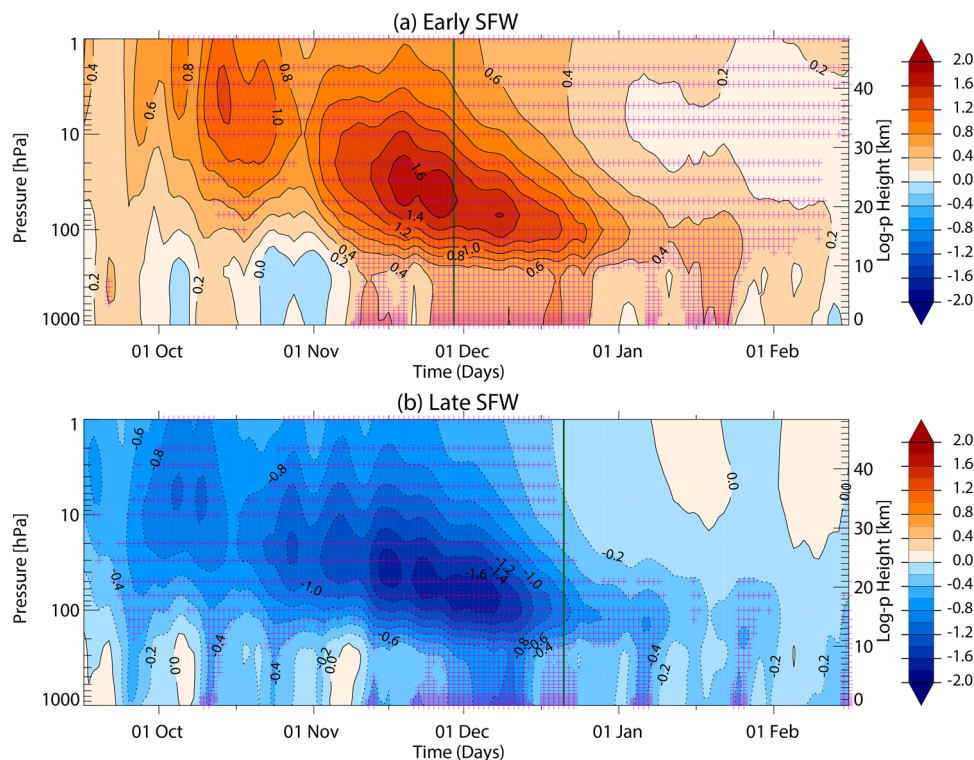


**Fig. 5** Cross-sections of time-height of PCH anomalies according to SFWOD. Composite of the PCH anomalies based on the calendar day of the year for **(a)** early-SFW and **(b)** late-SFW events. The green vertical line indicates the mean onset date of early and late-SFW events, respectively. Pink crosses indicate significant regions at the 95% confidence level.

date<sup>22</sup>. However, both early and late SFW events showed robust signals for the PCH anomaly in the troposphere and surface encompassing in December and January, especially in December. Surface responses during the summer (after December) appear closely linked with SFWOD, while those during the spring (before mid-November) are associated with the stratospheric polar vortex condition, especially early spring<sup>10</sup> (Supplementary Fig. 9 and Supplementary Note 4). Figure 5 shows that the surface weather in summer, shown in Fig. 2, was influenced by the timing of the final breakdown of the polar vortex via stratosphere-troposphere downward coupling.

The stratospheric PCH anomaly was used as an index of polar vortex<sup>21,26</sup>. Therefore, in the stratosphere during early spring (October–November), a positive PCH anomaly for early SFW events and a negative PCH anomaly for late SFW events indicated weakening and strengthening of the stratospheric polar vortex,

respectively. This confirms the results of a previous study on the association of the preceding stratospheric polar vortex condition with subsequent vortex breakdown events<sup>21</sup>.

**Discussion**

The cooling trend over the western and eastern Antarctic regions, which progressed until the end of the 20th century, paused or slightly reversed into a warming trend in the 21st century. The cessation of the Antarctic cooling occurred during summertime, but not in the wintertime. The trend change occurred around 1999, with a significant delay trend of SFWOD during the pre-1999 period but a significant advance trend during the post-1999 period, excluding the recent 3 years. Based on the examination using reanalysis data and in situ observations, we suggested that the trend differences in surface circulation and near-surface temperature over Antarctica during the austral summer season

are related to the trend toward earlier SFW occurrence since 1999. A significantly high MSLP anomaly appeared in the western Antarctic region for early SWF events, with warm SAT anomalies in the Amundsen Sea and west and east Antarctica. In contrast, for late SFW events, opposing or relatively weaker behaviors occurred. The distinctive surface weather patterns according to the SFWOD can be traced to the different downward influences from the stratosphere to the surface, although further studies are required to understand the detailed dynamic mechanisms for SFW timing and surface weather. The composite results for early SFW events were similar to the spatial patterns of the observed trend differences in the surface circulations between the delay and advance periods in the SFWOD. This resemblance implicitly reflects the strengthening of prominent surface circulation and near-surface temperature patterns during the austral summer for the early SFW events, since 1999. The differences in the congruent trends between the SFWOD delay and advance periods were similar to the spatial patterns of the observed trend differences in terms of their amplitudes and horizontal distribution, notably in the interior Antarctic region. This indicates that the long-term variability of the SFWOD is closely related to the observed trend differences in the regional SH surface climate. The resulting circulation changes appear to contribute considerably in the dipole anomalies of Antarctic SIC, with an increase over the AP region and a decrease over the northern Ross Sea.

The role of large-scale circulation linked to sea ice variability over the SH polar region has been examined in previous studies. Wang et al. (2021) showed the influence of SH polar vortex variability during austral spring on sea ice over the Ross and Weddell Seas, from austral spring to summer, through modulation of the Amundsen Sea Low via stratosphere-troposphere coupling<sup>15</sup>. However, Simpkins et al. (2012) reported that the proportion of SIC trends linearly attributable to the SAM was negligible<sup>27</sup>. In addition, Polvani et al. (2021) found little correlation between interannual variability and long-term trends in SIC around Antarctica and SAM<sup>28</sup>. The discrepant results among previous studies can be attributed in part to the periods or the spatial extent considered in the analysis; Supplementary Fig. 10 shows a positive SAM trend for the entire analysis period (1979–2017), however, its magnitude is only 30% compared to the SAM trend for the period before 1999 (1979–1999), and not statistically significant. Thus, the sea ice trend linearly congruent with the SAM trend, based on the entire analysis period, without considering the decadal variability in the surface circulation as shown in Simpkins et al.<sup>27</sup> can be small. Furthermore, the polar-cap-averaged sea ice as used in Polvani et al.<sup>28</sup> can show less prominent features through large cancellations between different sectors (Fig. 4). The results in Fig. 4, considering the decadal variability in atmospheric circulation and regional differences in sea ice response, may provide evidence for the above argument. The distribution of sea ice can also be affected by other factors, such as the phase transition of the Interdecadal Pacific Oscillation or the natural internal variability of atmospheric circulation<sup>1,16,29</sup>. Therefore, further investigation is required to understand the effects of the SFWOD-related atmospheric circulation on the long-term variability of sea ice, which is beyond the scope of this study.

The cause of the trend reversal in the SH SFWOD should be considered. Many studies have suggested an association between stratospheric ozone and the breakdown timing of the polar vortex during the austral summer<sup>20,22–25,30,31</sup>. The SH springtime ozone loss could lead to a colder and stronger polar vortex in the Antarctic stratosphere, through the reduced absorption of shortwave radiation. Consequently, the final breakdown date of the polar vortex can be delayed<sup>32,33</sup>. We confirmed that the relationship between Antarctic springtime ozone concentration

and SFWOD was consistent with previous studies. Figure 6 shows the long-term evolution of the amount of ozone and its seasonal evolution according to the SFW timing. The amount of total column ozone anomalies averaged over 65°S–90°S was used as a metric for Antarctic ozone. Figure 6a confirms the trend change in ozone levels around 2000, as previously reported<sup>15,34</sup>. The amount of total column ozone anomalies averaged from September to November (SON) significantly decreased during the pre-1999 period ( $-38.01$  DU decade<sup>-1</sup>) at the 95% confidence level. During the post-1999 period, however, there was a slightly positive trend in ozone concentration ( $1.94$  DU decade<sup>-1</sup>), although this was not statistically significant at the 95% confidence level. This pause or reversal in the ozone decline trend is consistent with the cessation of the delayed trend in SFWOD, and the slight warming in the summertime SAT anomaly over the west and east Antarctic regions from around 1999 to present, as shown in Fig. 1a. It was noteworthy that consistent ozone loss was observed in 2020, 2021, and 2022, which corresponded to the delayed onset of SFW. Studies to understand the cause of this ozone depletion have been reported<sup>35–37</sup>. It remains to be seen whether this is a temporary phenomenon or the beginning of a new long-term trend. The seasonal evolution of the total column ozone anomaly for early and late SFW events showed almost opposite evolution patterns based on a zero-value line from winter to summer (Fig. 6b). The positive and negative ozone values for early and late SFW started to increase from early spring, peaked in mid-to-late November, the period before the mean onset of SFWOD (gray vertical line), and then decreased rapidly. The significant negative relationship between the preceding ozone amount and the subsequent SFWOD on the seasonal timescale is further illustrated in Figure 6c<sup>22</sup>. The composite means of SON ozone anomalies for the early and late-SFW events were approximately 19.56 DU and  $-25.72$  DU, respectively, corresponding to more than half of one standard deviation of the SON ozone anomaly for 1979–2022 ( $1\sigma = 35$  DU) and statistically significant at the 95% confidence level. The anomalous behaviors in the stratospheric polar vortex during springtime, which were weaker for early SFWOD and stronger for late SFWOD (Fig. 5), were consistent with the amount of ozone according to the SFWOD. It is notable, however, that Fig. 6 does not show a causal relationship between ozone and SFWOD, nor does it indicate that ozone is the only factor that induces variability in a polar vortex. The amount of ozone in the stratosphere can also be affected by temperature changes and transport, owing to the dynamic process accompanying the breakdown of the polar vortex<sup>38</sup>.

The variability in the stratospheric polar vortex can also be modulated by other factors such as waves propagating from the troposphere, quasi-biennial oscillations, and El Niño–Southern Oscillations<sup>22,30,39–41</sup>. Although the increase in stratospheric ozone since the 21<sup>st</sup> century has weakened the polar vortex, the magnitudes of the polar vortex trends during the ozone recovery era have been reported as smaller than those during the ozone decline era<sup>13,42</sup>. Additionally, increased greenhouse gas emissions can offset the influence of ozone recovery by strengthening the polar vortex<sup>13,24</sup>. Rao and Garfinkel (2021) reported that a delay of SFW in the SH is projected in high emission scenarios using output of models, reflecting the important role of greenhouse gases<sup>24</sup>. Sun et al. (2014) showed that a robust downward influence on the troposphere was obtained only when there was a delay in the breakdown of the polar vortex, even though idealized ozone depletion was applied in the model<sup>20</sup>. Their results emphasized the important role of SFWOD in inducing variability in SH high-latitude surface weather conditions. Therefore, there are important considerations in predicting the long-term variability of the SFWOD and the resulting impacts on the surface

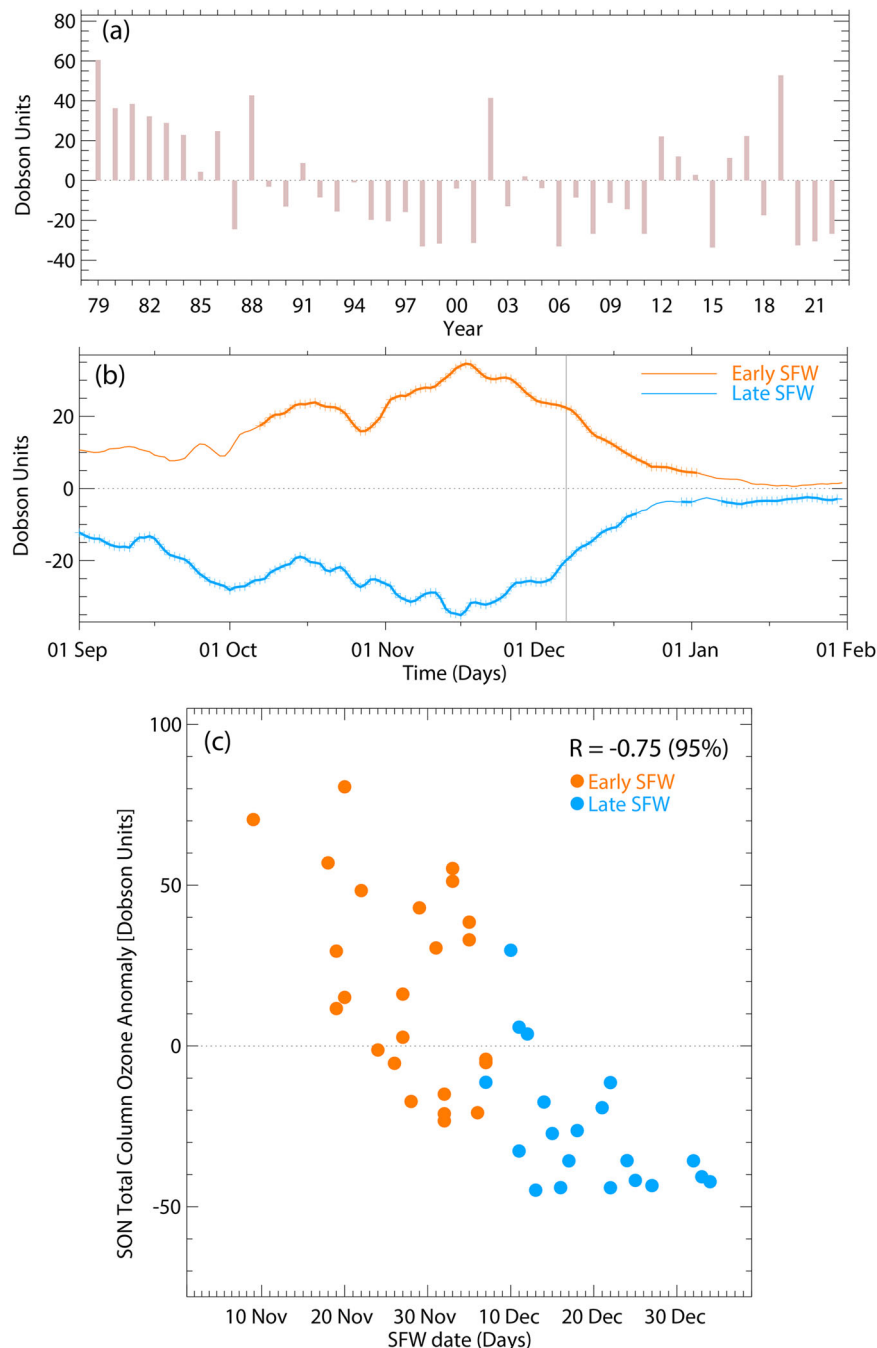


**Fig. 6 Time series of Antarctic ozone anomalies during springtime and the relationship between these anomalies and SFWOD.** **a** Time series of SON-mean total column ozone anomalies averaged over 65°S–90°S for 1979–2017. **b** Temporal evolution of composite mean SON-mean total column ozone anomalies averaged over 65°S–90°S for early- and late-SFW events. Orange and blue lines denote early and late-SFW events, respectively. The bold solid part of each line with crosses indicates statistically significant periods at the 95% confidence level. **c** Scatterplot of the SFW onset date against the SON-mean total column ozone anomalies averaged over 65°S–90°S. Orange and blue circles denote early- and late-SFW events, respectively. The correlation coefficient ( $R$ ) and confidence level (parentheses) are shown in the upper right corner of the plot.

climate by linking them with the increase in the amount of stratospheric ozone in recent decades.

In this study, the most important finding is that earlier SFWOD in the SH might lead to warmer Antarctic summers in recent decades. Congruence analyses support the potential role of SFWOD as a physical driver. A causal link, however, is not established by this work and more research is needed. Stratospheric anomalies associated with SFW events are observed more than 1 month ahead of summer tropospheric anomalies.

Therefore, a better understanding of SFW and its variability is crucial for improving the prediction of tropospheric climate and sea ice changes. We believe that this study could enrich the knowledge in the relevant field.

#### Methods

**Methods.** The SFWOD was identified as the last day that the zonal-mean zonal wind, smoothed by a 5-day running mean at 60°S and 50 hPa, dropped below  $10 \text{ m s}^{-1}$  until the following

austral autumn, based on the definition from Black and McDaniel<sup>19</sup>.

A composite analysis was conducted to identify the spatial patterns in the SH surface circulation according to the SFWOD. The SFWODs ranged from November 9 to January 3 with a mean onset date of December 8 based on the analysis period of this study<sup>19,22</sup>. The SFW events were classified into 24 early SFW events occurring before the mean SFWOD and 20 late SFW events occurring after the mean SFWOD (Supplementary Table 2). These events were used to investigate the characteristics of early and late SFW events. The mean onset date of early SFW events was November 28, approximately 3 weeks earlier than that of late SFW events, with a mean onset date of December 20. Note that we did not exclude cases that occurred very close to the mean date. We have confirmed that the relationship between SFWOD and surface response, however, is maintained regardless of the criteria dates for case classification, even though there are differences in intensity (not shown).

We examined the fraction of trends in surface circulation and temperature over the SH high-latitude regions, which are linearly congruent with the SFWOD. It was determined by regressing the DJ-mean values of MSLP and SAT anomalies onto SFWOD, and then multiplying the calculated regression coefficients by the SFWOD trend for the pre- and post-1999 periods, respectively.

The PCH anomaly was the geopotential height anomaly averaged over 65°S–90°S and normalized by its temporal standard deviation for the entire period at each pressure level. PCH was used to examine the stratosphere-troposphere downward coupling according to SFWOD. Statistical significance was determined from zero at the 90% and 95% confidence levels using the Student's *t*-test.

**Datasets.** All analyses based on reanalysis data were initially performed using the European Center for Medium Range Weather Forecasting Interim reanalysis (ERA-Interim) daily data from January 1, 1979, to August 31, 2018, with a horizontal resolution of 1.5° latitude × 1.5° longitude<sup>43,44</sup>. Regarding the main figures and some Supplementary Figures, we re-formed the analysis using the fifth generation of European Center for Medium Range Weather Forecasting reanalysis (ERA5) as a new replacement for ERA-interim from January 1, 1979, to March 31, 2023, with a horizontal resolution of 1° latitude × 1° longitude<sup>45</sup>. We use zonal wind and geopotential height at 37 pressure levels from 1000 to 1 hPa, MSLP, SAT at the 2-m level, and total column ozone from both reanalysis datasets. The anomaly fields were obtained from the deviation of the 31-day running mean climatological cycles, calculated from 1979 to 2017 for ERA-Interim and from 1979 to 2022 for ERA5. We have found that the main conclusions of this study are not sensitive to the different datasets and the inclusion of additional years, although there may be minor differences. Monthly mean SAT observations from January 1979 to January 2023 for 20 Antarctic stations provided by the Scientific Committee on Antarctic Research Reference Antarctic Data for Environmental Research database<sup>46</sup> were used for the composite analysis and trend of SAT over Antarctica (Supplementary Table 3). This monthly mean SAT was generated by averaging 6-hourly synoptic observations for which 90% of the data were available. The monthly SIC data from January 1979 to January 2022 were obtained from the National Snow and Ice Data Center, G02202.

### Data availability

All data used in this study are publicly accessible from these websites: ERA-Interim: <https://confluence.ecmwf.int/display/CKB/How+to+download+ERA-Interim+data+from+the+ECMWF+data+archive>, ERA5 dataset: <https://cds.climate.copernicus.eu/>

[cdsapp#!/dataset/reanalysis-era5-single-levels?tab=overview](https://cdsapp#!/dataset/reanalysis-era5-single-levels?tab=overview), SAM index: [https://www.cpc.ncep.noaa.gov/products/precip/CWlink/daily\\_ao\\_index/ao/ao.shtml](https://www.cpc.ncep.noaa.gov/products/precip/CWlink/daily_ao_index/ao/ao.shtml), Scientific Committee on Antarctic Research Reference Antarctic Data for Environmental Research database: <https://legacy.bas.ac.uk/met/READER/data.html> and National Snow and Ice Data Center SIC: [https://noaadata.apps.nsidc.org/NOAA/G02202\\_V4/south/monthly/](https://noaadata.apps.nsidc.org/NOAA/G02202_V4/south/monthly/).

### Code availability

All figures were created with the Interactive Data Language (IDL)<sup>47</sup>. The Climate Data Operator (CDO) software was also utilized manipulating and analyzing climate data<sup>48</sup>. All codes used in this study are available upon request.

Received: 11 May 2023; Accepted: 12 January 2024;

Published online: 24 January 2024

### References

- Turner, J., Hosking, J. S., Marshall, G. J., Phillips, T. & Bracegirdle, T. J. Antarctic sea ice increase consistent with intrinsic variability of the Amundsen Sea Low. *Clim. Dynam.* **46**, 2391–240 (2016).
- Paolo, F. S. et al. Response of Pacific-sector Antarctic ice shelves to the El Niño/Southern oscillation. *Nat. Geosci.* **11**, 121–126 (2018).
- Pörtner, H. O. et al. The ocean and cryosphere in a changing climate. *IPCC Special Report on the Ocean and Cryosphere in a Changing Climate* (2019).
- Rignot, E. et al. Four decades of Antarctic Ice Sheet mass balance from 1979–2017. *Proc. Natl Acad. Sci. USA* **116**, 1095–1103 (2019).
- Masson-Delmotte, V. et al. Climate change 2021: the physical science basis. Contribution of Working Group I to the Sixth Assessment Report of the Intergovernmental Panel on Climate Change. *IPCC: Geneva, Switzerland* (2021).
- Massom, R. A. et al. Antarctic ice shelf disintegration triggered by sea ice loss and ocean swell. *Nature* **558**, 383–389 (2018).
- Riihelä, A., Bright, R. M. & Anttila, K. Recent strengthening of snow and ice albedo feedback driven by Antarctic sea-ice loss. *Nat. Geosci.* **14**, 832–836 (2021).
- England, M. R., Polvani, L. M., Sun, L. & Deser, C. Tropical climate responses to projected Arctic and Antarctic sea-ice loss. *Nat. Geosci.* **13**, 275–281 (2020a).
- England, M. R., Polvani, L. M. & Sun, L. Robust Arctic warming caused by projected Antarctic sea ice loss. *Environ. Res. Lett.* **15**, 104005 (2020b).
- Kwon, H., Choi, H., Kim, B. M., Kim, S. W. & Kim, S. J. Recent weakening of the southern stratospheric polar vortex and its impact on the surface climate over Antarctica. *Environ. Res. Lett.* **15**, 094072 (2020).
- Jun, S. Y. et al. The internal origin of the west-east asymmetry of Antarctic climate change. *Sci. Adv.* **6**, eaazi1490 (2020).
- England, M. R., Polvani, L. M., Smith, K. L., Landrum, L. & Holland, M. M. Robust response of the Amundsen Sea Low to stratospheric ozone depletion. *Geophys. Res. Lett.* **43**, 8207–8213 (2016).
- Banerjee, A., Fyfe, J. C., Polvani, L. M., Waugh, D. & Chang, K. L. A pause in Southern Hemisphere circulation trends due to the Montreal Protocol. *Nature* **579**, 544–548 (2020).
- Clem, K. R. et al. Record warming at the South Pole during the past three decades. *Nat. Clim. Change* **10**, 762–770 (2020).
- Wang, S. et al. How do weakening of the stratospheric polar vortex in the southern hemisphere affect regional Antarctic Sea ice extent? *Geophys. Res. Lett.* **48**, e2021GL092582 (2021).
- Chung, E. S. et al. Antarctic sea-ice expansion and Southern Ocean cooling linked to tropical variability. *Nat. Clim. Change* **12**, 461–468 (2022).
- Rahaman, W., Chatterjee, S., Ejaz, T. & Thamban, M. Increased influence of ENSO on Antarctic temperature since the Industrial Era. *Sci. Rep.* **9**, 6006 (2019).
- Turner, J. et al. Antarctic temperature variability and change from station data. *Int. J. Climatol.* **40**, 2986–3007 (2020).
- Black, R. X. & McDaniel, B. A. Interannual variability in the Southern Hemisphere circulation organized by stratospheric final warming events. *J. Atmos. Sci.* **64**, 2968–2974 (2007).
- Sun, L., Chen, G. & Robinson, W. A. The role of stratospheric polar vortex breakdown in Southern Hemisphere climate trends. *J. Atmos. Sci.* **71**, 2335–2353 (2014).
- Byrne, N. J. & Shepherd, T. G. Seasonal persistence of circulation anomalies in the Southern Hemisphere stratosphere and its implications for the troposphere. *J. Clim.* **31**, 3467–3483 (2018).
- Butler, A. H. & Domeisen, D. I. The wave geometry of final stratospheric warming events. *Weather Clim. Dyn.* **2**, 453–474 (2021).
- Byrne, N. J., Shepherd, T. G., Woollings, T. & Plumb, R. A. Nonstationarity in Southern Hemisphere climate variability associated with the seasonal breakdown of the stratospheric polar vortex. *J. Clim.* **30**, 7125–7139 (2017).



24. Rao, J. & Garfinkel, C. I. Projected changes of stratospheric final warmings in the Northern and Southern Hemispheres by CMIP5/6 models. *Clim. Dyn.* **56**, 3353–3371 (2021).
25. Hirano, S., Kohma, M. & Sato, K. A three-dimensional analysis on the role of atmospheric waves in the climatology and interannual variability of stratospheric final warming in the Southern Hemisphere. *J. Geophys. Res. Atmos.* **121**, 8429–8443 (2016).
26. Rao, J., Garfinkel, C. I., Wu, T., Lu, Y. & Chu, M. Mean state of the Northern Hemisphere stratospheric polar vortex in three generations of CMIP models. *J. Clim.* **35**, 1–49 (2022).
27. Simpkins, G. R., Ciasto, L. M., Thompson, D. W. & England, M. H. Seasonal relationships between large-scale climate variability and Antarctic sea ice concentration. *J. Clim.* **25**, 5451–5469 (2012).
28. Polvani, L. M. et al. Interannual SAM modulation of Antarctic Sea ice extent does not account for its long-term trends, pointing to a limited role for ozone depletion. *Geophys. Res. Lett.* **48**, e2021GL094871 (2021).
29. Meehl, G. A. et al. Sustained ocean changes contributed to sudden Antarctic sea ice retreat in late 2016. *Nat. Commun.* **10**, 14 (2019).
30. Haigh, J. D. & Roscoe, H. K. The final warming date of the Antarctic polar vortex and influences on its interannual variability. *J. Clim.* **22**, 5809–5819 (2009).
31. Sheshadri, A., Plumb, R. A. & Domeisen, D. I. Can the delay in Antarctic polar vortex breakup explain recent trends in surface westerlies? *J. Atmos. Sci.* **71**, 566–573 (2014).
32. Zhou, S., Gelman, M. E., Miller, A. J. & McCormack, J. P. An inter-hemisphere comparison of the persistent stratospheric polar vortex. *Geophys. Res. Lett.* **27**, 1123–1126 (2000).
33. Thompson, D. W. et al. Signatures of the Antarctic ozone hole in Southern Hemisphere surface climate change. *Nat. Geosci.* **4**, 741–749 (2011).
34. Solomon, S. et al. Emergence of healing in the Antarctic ozone layer. *Science* **353**, 269–274 (2016).
35. Ansmann, A. et al. Ozone depletion in the Arctic and Antarctic stratosphere induced by wildfire smoke. *Atmos. Chem. Phys.* **22**, 11701–11726 (2022).
36. Zhu, Y. et al. Perturbations in stratospheric aerosol evolution due to the water-rich plume of the 2022 Hunga-Tonga eruption. *Commun. Earth Environ.* **3**, 248 (2022).
37. Manney, G. L. et al. Siege in the southern stratosphere: Hunga Tonga-Hunga Ha’apai water vapor excluded from the 2022 Antarctic polar vortex. *Geophys. Res. Lett.* **50**, e2023GL103855 (2023).
38. Manney, G. L. & Lawrence, Z. D. The major stratospheric final warming in 2016: dispersal of vortex air and termination of Arctic chemical ozone loss. *Atmos. Chem. Phys.* **16**, 15371–15396 (2016).
39. Baldwin, M. P. & Dunkerton, T. J. Quasi-biennial modulation of the southern hemisphere stratospheric polar vortex. *Geophys. Res. Lett.* **25**, 3343–3346 (1998).
40. Stone, K. A., Solomon, S., Thompson, D. W., Kinnison, D. E. & Fyfe, J. C. On the Southern Hemisphere stratospheric response to ENSO and its impacts on tropospheric circulation. *J. Clim.* **35**, 1963–1981 (2022).
41. Hirano, S., Kohma, M. & Sato, K. Interannual variability of stratospheric final warming in the Southern Hemisphere and its tropospheric origin. *J. Clim.* **34**, 6115–6128 (2021).
42. Zambri, B., Solomon, S., Thompson, D. W. & Fu, Q. Emergence of Southern Hemisphere stratospheric circulation changes in response to ozone recovery. *Nat. Geosci.* **14**, 638–644 (2021).
43. Dee, D. P. et al. The ERA-Interim reanalysis: configuration and performance of the data assimilation system. *Q. J. R. Meteorol. Soc.* **137**, 553–597 (2011).
44. Bracegirdle, T. J. & Marshall, G. J. The reliability of Antarctic tropospheric pressure and temperature in the latest global reanalyses. *J. Clim.* **25**, 7138–7146 (2012).
45. Tetzner, D., Thomas, E. & Allen, C. A validation of ERA5 reanalysis data in the Southern Antarctic Peninsula—Ellsworth land region, and its implications for ice core studies. *Geosciences* **9**, 289 (2019).
46. Turner, J. et al. The SCAR READER project: toward a high-quality database of mean Antarctic meteorological observations. *J. Clim.* **17**, 2890–2898 (2004).
47. Bowman, K. P. *An Introduction to Programming with IDL: Interactive Data Language* (Elsevier, 2006).
48. Schulzweida, U. CDO user guide. Zenodo. <https://doi.org/10.5281/zenodo.3539275> (2019).

### Acknowledgements

Korea Polar Research Institute “Understanding of Antarctic climate and environment and assessments of global influence” project (PE24030) funded by the Ministry of Oceans and Fisheries. This work was supported by the National Research Foundation of Korea (NRF) grant funded by the Korea government (MSIT) (No. NRF-2022R1A2C1006788). H.K. was supported by the National Research Foundation of Korea (NRF) grant funded by the Korea government (NRF-2023R1A2C1008238)

### Author contributions

H.C., S.K., and B.K. conceived and developed the initial idea for the study. H.C. and S.K. designed the research methodology. H.C. and H.K. conducted the investigation and collected data. H.C. and H.K. created visualizations for the data. S.K. and B.K. supervised the overall progress of the study. H.C., S.K., B.K., and H.K. contributed to the writing of the manuscript.

### Competing interests

The authors declare no competing interests.

### Additional information

**Supplementary information** The online version contains supplementary material available at <https://doi.org/10.1038/s43247-024-01221-0>.

**Correspondence** and requests for materials should be addressed to Seong-Joong Kim or Baek-Min Kim.

**Peer review information** *Communications Earth & Environment* thanks the anonymous reviewers for their contribution to the peer review of this work. Primary Handling Editors: Mengze Li, Heike Langenberg. A peer review file is available.

**Reprints and permission information** is available at <http://www.nature.com/reprints>

**Publisher’s note** Springer Nature remains neutral with regard to jurisdictional claims in published maps and institutional affiliations.



**Open Access** This article is licensed under a Creative Commons Attribution 4.0 International License, which permits use, sharing, adaptation, distribution and reproduction in any medium or format, as long as you give appropriate credit to the original author(s) and the source, provide a link to the Creative Commons licence, and indicate if changes were made. The images or other third party material in this article are included in the article’s Creative Commons licence, unless indicated otherwise in a credit line to the material. If material is not included in the article’s Creative Commons licence and your intended use is not permitted by statutory regulation or exceeds the permitted use, you will need to obtain permission directly from the copyright holder. To view a copy of this licence, visit <http://creativecommons.org/licenses/by/4.0/>.

© The Author(s) 2024